Letters in Applied NanoBioScience
Open-Access Journal (ISSN: 2284-6808)

Article
Volume 15, Issue 2, 2026, 68
https://doi.org/10.33263/LIANBS152.068

Antioxidant and Antidiabetic Activities of Green Synthesized ZnO Nanoparticles Using Fresh and Dried Leaf Extracts of *Annona squamosa*

Sharon Min Suan Chiew [1], Hartini Mohd Yasin [1], Ai Ling Tan [1,*]

[1] Faculty of Science, Universiti Brunei Darussalam, Jalan Tungku Link, Gadong, BE1410, Brunei Darussalam
* Correspondence: ailing.tan@ubd.edu.bn;

Received: 14.03.2025; Accepted: 24.02.2026; Published: 30.06.2026

Abstract: Green-synthesized nanoparticles have gained significant attention in recent years due to their unique functional properties, particularly for disease treatment and in enhancing antioxidant activity for food and cosmetic applications. In this study, zinc oxide nanoparticles (ZnO NPs) were synthesized using fresh (ZnO-FH and ZnO-FS) and dried (ZnO-DS) leaf extracts of Annona squamosa through different approaches. The nanoparticles were characterized using FTIR, SEM, and XRD techniques. FTIR analysis confirmed the presence of organic functional groups responsible for the nanoparticle formation. XRD analysis showed their average crystallite size to be 11 nm. SEM images showed that ZnO-FH and ZnO-FS formed agglomerated spherical particles, while ZnO-DS exhibited a coral-like structure surrounded by spherical particles, with average particle size ranging from 68 to 111 nm. Preliminary phytochemical screening of these nanomaterials was conducted. Antioxidant activity of both extracts and nanoparticles was evaluated using DPPH free radical scavenging and ferric reducing power assays. The dried leaf extract demonstrated the strongest DPPH radical scavenging and reducing power, while ZnO-DS exhibited the highest radical scavenging activity at the highest concentration tested. In addition, α-glucosidase inhibition assays showed that both the leaf extracts and ZnO-DS displayed the strongest enzyme inhibition activity. Overall, this study shows that dried leaf extracts and ZnO-DS possess the highest antioxidant and antidiabetic potential.

Keywords: *Annona squamosa*; zinc oxide nanoparticles; antioxidant; antidiabetic.

1. Introduction

In recent decades, nanoparticles have been employed in many different scopes, including molecular biology, chemistry, material science, and medical applications [1]. Nanoparticles (NPs) are particularly useful in the diagnosis and treatment of certain diseases, as they can selectively permeate biological barriers, specifically identify and assemble at targeted diseased cells or tissues [2]. Hence, they have multifunctional roles in numerous biomedical applications. Among metal oxide nanoparticles, ZnO NPs are relatively cheap, biocompatible, mechanically stable, and easily surface-modified, making them highly suitable for biomedical applications [3]. Green-synthesized ZnO, derived from plant and microorganism extracts, has gained popularity due to its simplicity, high yields, low toxicity, cost-effectiveness, and environmental benefits, outpacing non-green preparation approaches [4]. Secondary metabolites involved in plant metabolic pathways, such as phenolic acids,

terpenoids, and alkaloids, can act as reducing and capping agents, leading to the formation of stable nanoparticles [5]. ZnO NPs are known to exhibit effective activities as an antioxidant [5,6], antidiabetic [6,7], antibacterial [6,8], and anticancer agent [9] as they can interact effectively with biological membranes.

ZnO NPs prepared from leaf extracts of *Azadirachta indica*, *Hibiscus rosa-sinensis*, *Murraya koenigii*, *Moringa oleifera*, and *Tamarindus indica* [10] exhibited high antioxidant, α-amylase, and α-glucosidase inhibitory activities, whereas *Erythrina variegata* [11], *Eucalyptus globulus* [12], and *Ziziphus mauritiana* Lam [4] were reported to exhibit high percentage of 2,2-diphenyl-1-picrylhydrazyl (DPPH) radical inhibition. The antioxidant activity of green-synthesized ZnO NPs is mainly attributed to phytochemicals in the plant extracts, which act as hydrogen donors, along with the intrinsic free radical scavenging ability of ZnO. Owing to its good glucose tolerance and insulin sensitivity, ZnO is considered a promising antidiabetic agent. It can bind with α-amylase and α-glucosidase, inhibiting their activity and thereby reducing blood glucose level [13]. With the rapid increase in diabetes mellitus cases over the past several decades, it has become a major global public health concern. Thus, the development of bio-safe ZnO NPs as antidiabetic agents is strongly recommended to help regulate glucose and insulin mechanisms [14].

Annona squamosa Linn. (Figure 1) is a member of the Annonaceae family, which bears edible fruit commonly known as sugar apple, custard apple, or sweet sop. In folkloric medicine, there have been reports of the applications of A. squamosa as an anticancer, antidiabetic, antioxidant, antilipidemic, and anti-inflammatory agent, which have been verified by recent research [15,16]. Traditionally, the leaf extract of this plant is crushed and applied to wounds[17], treatment of urinary tract infection and dysentery [18], a cold and cough remedy, and used to treat intestinal infections [19]. Phytochemical screening of the aqueous leaf extract showed the presence of glycosides, oils, saponins, phenols, and flavonoids [20]. The high content of phenolic and flavonoid compounds present in the plant extract contributed strongly to the fact that *A. squamosa* possessed exceptional antioxidant and antidiabetic properties [21].

Figure 1. (a) *A. squamosa* Linn. fruit and leaves; **(b)** *A. squamosa* Linn. leaf.

Although *A. squamosa* is widely used as a remedial agent, the literature review revealed that the green synthesis of ZnO NPs from this plant and its potential applications remain unexplored. The aim of this study was to synthesize ZnO NPs using *A. squamosa* leaf extract and water as the extraction solvent, with the phytochemicals in the extract serving as both reducing and capping agents. The green-synthesized ZnO NPs and the leaf extract were prepared from both fresh and dried leaves by heating at 60°C or by sonicating at room temperature. Fresh plant extracts contain more water and volatile phytochemicals, while dried

extracts contain more concentrated, stable phytochemicals that may lead to different nanoparticle formation. All synthesized compounds were then characterized using FT-IR (Fourier transform infrared), SEM (Scanning Electron Microscopy), and XRD (X-ray diffraction) techniques. Antioxidant properties of the synthesized compounds and extracts were evaluated based on phenolic content using Folin-Ciocalteu reagent, flavonoid content via the aluminum chloride method, DPPH radical scavenging activity, and ferric reducing antioxidant power (FRAP) assays. This paper also reported the *in vitro* antidiabetic activity of the samples using an α-glucosidase inhibitory assay.

2. Materials and Methods

A. squamosa leaves were collected from the Tutong district, Brunei Darussalam. Zinc nitrate hexahydrate (98.0%), commercial zinc oxide, iodine, quercetin (≥ 95.0%), di-sodium hydrogen phosphate heptahydrate, and potassium acetate (≥ 99.0%) were all purchased from Sigma-Aldrich. Methanol (≥ 99.5%), sodium carbonate, sodium acetate (99.0%), aluminum chloride (97.0% – 101.0%), gallic acid, Folin-Ciocalteu reagent, and dimethyl sulfoxide (≥ 99.9%) were obtained from Merck. Other reagents used include 1,1-diphenyl-2-picrylhydrazyl (97.0%) from Tokyo Chemical Industry Co. Ltd., sodium dihydrogen orthophosphate (99.0%) from Ajax Chemicals, potassium ferricyanide (99.0%) from AnalaR, ferric chloride (99.0%) from R&M Chemicals, glacial acetic acid (99.8%) from Merck Pro Analysis, trichloroacetic acid (≥ 99.0%) and ferrous sulfate (≥ 99.5%) from Fluka. Fourier transform infrared spectroscopy (FTIR, Shimadzu IR Prestige-21 Fourier Transform Infrared Spectrometer) was used to identify the functional and phytochemical constituents of the leaf extracts and ZnO NPs. Morphology and size of nanoparticles were analyzed with FESEM (JSM-7610 JEOL JAPAN) and Shimadzu XRD-7000. A single beam UV-Visible spectrophotometer (UV-Vis, Thermo Scientific Genesys 20) was used to monitor the absorbance for the antioxidant assays. A microplate reader (Biobase Elisa Microplate Reader, BK-EL10C) was employed for the determination of antidiabetic activity.

2.1. Preparation of leaf extract.

Three different methods of preparing the leaf extract of *A. squamosa* are reported herein: methods A, B, and C (Figure 2). For methods A and B, the leaves of *A. squamosa* were washed with tap water, and the fresh leaves were cut, blended, and ground. 200 mL of distilled water was then added to 20 g of ground leaves. In method A, the mixture was heated at 60°C for 1 h with stirring, whereas in method B, the mixture was sonicated at room temperature for 30 mins. A different approach was carried out for method C; the leaves were dehydrated for 7 h and then ground and sieved using a 710-micron mesh. 200 mL of distilled water was then added to 20 g of dried powder leaves, and the mixture was sonicated at room temperature for 30 minutes. In all three methods, the extract was obtained by vacuum filtration. The leaf extract prepared was used directly to synthesize ZnO.

For preparation of the freeze-dried leaf extract of *A. squamosa*, the aqueous leaf extract was dehydrated to half its initial volume, then freeze-dried for 3 days. The freeze-dried extracts obtained were labeled LE-FH (method A), LE-FS (method B), and LE-DS (method C) and stored in a desiccator until further use. Figure 2 summarizes all methods used to obtain the leaf extracts and ZnO NPs products for this work.

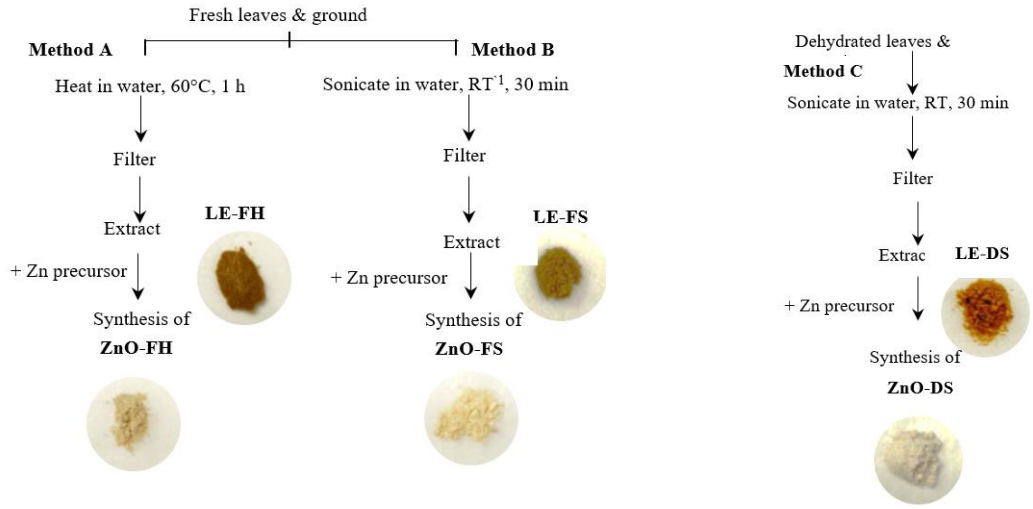

[1]RT = room temperature

Figure 2. Summary of the methods used for the synthesis of ZnO.

2.2. Preparation of ZnO NPs using aqueous leaf extract of A. squamosa.

1 g of $Zn(NO_3)_2.6H_2O$ (0.067 M) was added to 50 mL of aqueous leaf extract, and the solution was heated at 80°C with stirring until a dark brown paste was observed. The paste was then transferred into a crucible and calcined at 400°C for 2 h. The powder was ground finely and labeled as ZnO-FH (method A), ZnO-FS (method B), and ZnO-DS (method C) and stored in a desiccator until further use.

2.3. Phytochemical studies.

The phytochemicals in the leaf extract and the green-synthesized ZnO NPs were analyzed following the protocol reported by Shaikh and Patil, with slight modifications [22]. For sample preparation prior to qualitative analysis of bioactive compounds, both ZnO NPs and the leaf extracts dissolved in water were sonicated at room temperature for 15 minutes, followed by centrifugation at 3500 rpm for 5 minutes. Table 1 shows the procedure for each phytochemical test and the expected observation for a positive result.

Table 1. Qualitative tests for preliminary phytochemical screening.

Phytochemical	Test	Procedure	Observation (Positive)
Alkaloid	Iodine test	3 mL sample solution + a few drops of I_2 solution.	Blue color disappears on boiling and reappears on cooling.
Quinones	Conc. HCl test	Extract + Conc. HCl.	Green colour.
Saponins	Foam test	Extract + 2 mL water (vigorously shaken).	Persistent foam for 10 mins.
Flavonoids	Ferric chloride test	Sample solution + a few drops of 10% $FeCl_3$ solution.	Green precipitate.
Phenols	Iodine test	1 mL sample solution + a few drops of diluted I_2 solution.	Transient red color.
Tannins	Braymer's test	1 mL sample solution + 3 mL water + 3 drops of 10% $FeCl_3$ solution.	Blue-green colour.
Glycosides	Sodium hydroxide test	Alcoholic sample extract + Dissolved in water + A few drops of NaOH.	Yellow colour.
Keller-Killani test	Sodium hydroxide test	Sample extract + 1.5 mL glacial CH_3COOH + 1 drop of 5% $FeCl_3$ + Conc. H_2SO_4 (along the side of the test tube).	Blue color in the acetic acid layer.

2.4. Antioxidant studies.

Four antioxidant studies of the *A. squamosa* fabricated ZnO NPs and leaf extracts were performed. The antioxidant properties of the synthesized samples and extracts were evaluated by determining the total phenolic content using Folin-Ciocalteu reagent, total flavonoid content using aluminum chloride assay, DPPH free radical scavenging activity, and ferric reducing antioxidant power (FRAP) assay. The antioxidant experiments were performed in triplicate.

The total phenolic content was determined by the Folin-Ciocalteu assays following the procedure reported by Badrulhisham *et al*. [23] with slight modifications. 0.5 mL of sample (1000 ppm) was mixed with 2.5 mL of 10% Folin-Ciocalteu solution and left for 5 minutes of incubation in the dark at room temperature. 2.0 mL of 7.5% sodium carbonate solution was then added, and the mixture was mixed on a vortex followed by incubation for 30 minutes at room temperature. The absorbance was measured at 765 nm with 80% (v/v) methanol as a blank. The total phenolic content was determined from the standard calibration curve of gallic acid for concentrations ranging between 0 and 100 ppm. The TPC was calculated from the following equation (1) and expressed as milligrams of gallic acid equivalent per gram of crude extract (mg GAE/g crude extract) [24].

$$TPC\ (mg\ GAE/g\ crude\ extract) = \frac{c \times V}{m} \qquad (1)$$

Where c is the gallic acid concentration (in mg/L) established from the calibration curve, V is the sample volume (in L), and m is the weight of the sample dry matter (g).

The total flavonoid content was determined by a colorimetric assay using aluminum chloride in accordance with the protocol reported by Borrás-Linares *et al*. [25], with slight modifications. 0.5 mL of sample (1000 ppm) was mixed with 0.1 mL of 10% (v/v) aluminum chloride solution, 0.1 mL of potassium acetate solution, 1.5 mL of ethanol, and 2.8 mL of distilled water. The mixture was mixed on a vortex followed by incubation in the dark for 30 minutes at room temperature. The absorbance of the resultant mixture was measured at 415 nm with 80% (v/v) methanol as a blank. The total flavonoid content was determined from the standard calibration of quercetin (0 – 100 ppm). The TFC was calculated from the following equation (2) and expressed as milligrams of quercetin equivalent per gram of crude extract (mg QE/g crude extract) [26].

$$TFC\ (mg\ QE/g\ crude\ extract) = \frac{c \times V}{m} \qquad (2)$$

Where c is the quercetin concentration (in mg/L) obtained from the standard quercetin calibration curve, V is the sample volume (in L), and m is the weight of the sample dry matter (in g).

The antioxidant activity was assessed via free radical scavenging activity of the samples using the stable 1,1-diphenyl-2-picrylhydrazyl (DPPH) radicals following the method as described by Brand-Williams with some modifications [27]. 2 mL of DPPH was added to 1 mL of the sample, and the solution was stirred for 30 minutes at room temperature in the dark. After 30 minutes of incubation, the sample was centrifuged, and the supernatant was used for analysis by measuring the absorbance at 514 nm. Ascorbic acid was used as the standard, and a solution containing only DPPH was used as the control. The radical scavenging activity (%) was evaluated using the following equation (3) [28]:

$$Radical\ scavenging\ activity\ (\%) = \frac{A_0 - A_1}{A_0} \times 100 \qquad (3)$$

Where A0 is the absorbance of the control solution, and A1 is the absorbance of the sample/standard solution. The IC_{50} value was obtained from the DPPH calibration graph of the respective sample within a concentration range.

The iron-reducing power property of the samples was evaluated using the procedure reported by Motazedi *et al*. [29] with slight modifications. 1 mL of 100 ppm of each sample was mixed with a solution containing 1 mL of phosphate buffer (0.2 M, pH 6.8) and 1 mL of potassium ferricyanide (1.0% w/v). The solution was then incubated at 50°C for 20 minutes in a water bath. The solution was then allowed to cool to room temperature, followed by the addition of 0.5 mL of trichloroacetic acid (10% v/v). After centrifugation for 5 mins, 1 mL of supernatant was mixed with 1 mL of distilled water and 0.6 mL of ferric chloride (0.1% w/v). Ascorbic acid was used as the positive control, ferrous sulfate as the standard, and the absorbance was measured at 700 nm. The FRAP value was determined using the following equation (4) and expressed as milligrams of ferrous sulfate equivalent per gram of crude extract (mg FSE/g crude extract) [30].

$$FRAP\ value\ (mg\ FSE/g\ crude\ extract) = \frac{c \times V \times t}{m} \qquad (4)$$

Where c is the ferrous sulfate concentration (in mg/L) obtained from the standard calibration curve, V is the sample volume (in L), t is the dilution factor, and m is the weight of the sample dry matter (in g).

2.5. Antidiabetic studies.

An *in vitro* antidiabetic analysis of the ZnO NPs synthesized from *A. squamosa* leaf extracts was conducted via α-glucosidase inhibition assay. α-glucosidase inhibition activity was performed following the protocol as outlined by Lankatillake *et al*. [31], with some modifications. 100 ppm of acarbose, and samples were prepared using 10% (v/v) DMSO. 50 µL of each sample, acarbose (positive control), and phosphate buffer (negative control) were transferred into the sample wells. An additional 50 µL of phosphate buffer was added to those wells, followed by the addition of 30 µL of α-glucosidase enzyme. The solutions were incubated in the dark at 37°C for 10 minutes. The reaction was started by the addition of 20 µL of p-nitrophenol-α-glucopyranoside (pNPG) substrate and incubated for another 20 minutes. The reaction was stopped with the addition of 100 µL of Na_2CO_3. Samples well with 80 µL phosphate buffer and 20 µL pNPG substrate were set as a blank. The absorbance was measured at 405 nm, and the percentage enzyme inhibition was calculated as follows: equation (5):

$$\propto -glucosidase\ inhibition\ (\%) = \frac{A_{nc} - A_s}{A_{nc}} \times 100 \qquad (5)$$

Where A_{nc} is the absorbance of the negative control and A_s is the absorbance of the sample or positive control, the antidiabetic experiments were performed in triplicate.

3. Results and Discussion

3.1. Characterization of leaf extracts and ZnO.

FTIR analysis was conducted to determine the functional groups responsible for the reduction of zinc nitrate to zinc oxide and for the stabilization of the synthesized nanoparticles.

The samples, which included the leaf extracts (LE-FH, LE-FS, LE-DS), biosynthesized ZnO NPs (ZnO-FH, ZnO-FS, ZnO-DS), and commercial ZnO (C-ZnO), were all examined using FTIR spectroscopy in the range of 4000 – 400 cm^{-1}. Figure 3a illustrates the FTIR spectra of commercial ZnO (C-ZnO), a sample synthesized using the dried leaves (ZnO-DS) and dried leaves extract (LE-DS). The FTIR analysis of the dried leaf extracts (LE-DS) displayed peaks at 3384 cm^{-1} and 1410 cm^{-1} corresponding to O–H stretching and bending, respectively. The O–H stretching may be due to the presence of moisture, whereas the O–H bending vibration may be owing to the presence of flavonoids and reducing sugars in the plant extract [4,32]. There are also two other peaks at 1629 cm^{-1} and 1047 cm^{-1} attributed to C=O of carbonyl group and C–N, respectively [33,34]. All the IR bands observed in LE-DS confirmed that A. squamosa leaves are saturated with various phytochemicals, including phenolic compounds, flavonoids, and proteins [35]. The green synthesized ZnO NPs (ZnO-DS) possessed similar functional groups as the dried leaf extracts (LE-DS). These results proved that the phytochemicals present in *A. squamosa* leaves were capped onto the surface of the ZnO samples during synthesis. In addition, ZnO-DS possessed two extra peaks at 872 cm^{-1} and 473 cm^{-1} attributed to Zn–OH and Zn–O, respectively. This justified the successful synthesis of ZnO NPs [32].The IR peak of Zn–O at 471 cm^{-1} in the commercial ZnO further confirms the presence of Zn–O in the synthesized nanoparticles sample.

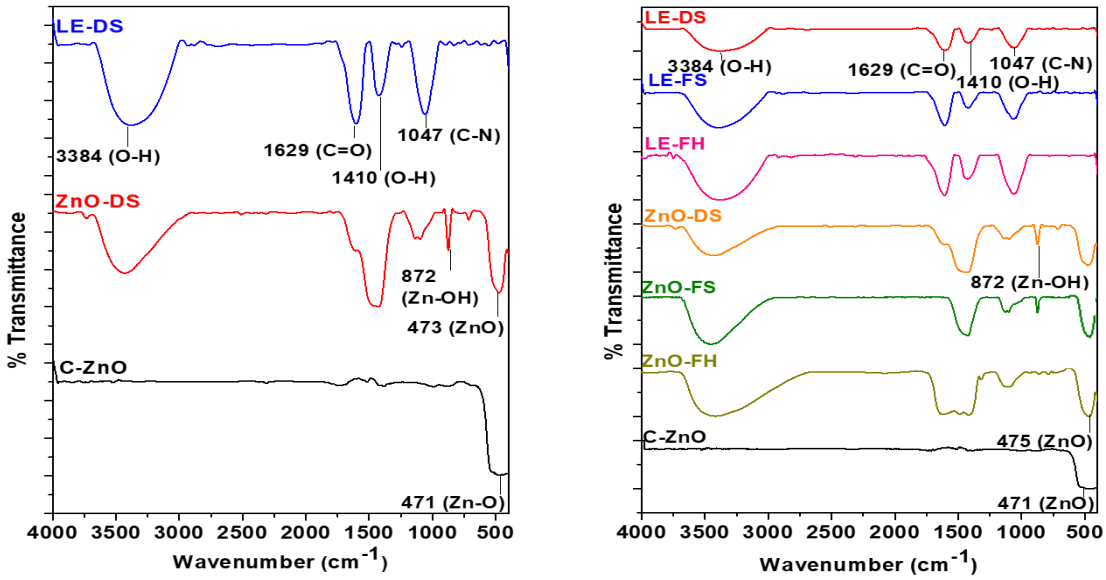

Figure 3. FTIR spectra of **(a)** leaf extracts (LE-DS), biosynthesized ZnO NPs (ZnO-DS), and commercial ZnO (C-ZnO); **(b)** leaf extracts (LE-FH, LE-FS, LE-DS), biosynthesized ZnO NPs (ZnO-FH, ZnO-FS, ZnO-DS), and commercial ZnO (C-ZnO).

Figure 3b demonstrates the FTIR spectra of commercial ZnO and all the synthesized nanoparticles and leaf extracts. Between the different samples of leaf extracts (LE-FH, LE-FS, and LE-DS), all three leaf extract samples demonstrated four IR peaks at ~3400 cm^{-1}, ~1620 cm^{-1}, ~1400 cm^{-1}, and ~1040 cm^{-1} corresponding to O–H stretch, C=O of carbonyls, O–H bend, and C–N, respectively. The presence of these functional groups verified that *A. squamosa* leaves are rich in phytochemicals, including phenolics, flavonoids, and proteins, regardless of the extraction method [4,32–34].

Among the different samples of ZnO NPs (ZnO-FH, ZnO-FS, ZnO-DS), all three synthesized samples exhibited Zn–O peak at ~470 cm^{-1}, O–H stretch at ~3400 cm^{-1}, and O–H bend at ~1400 cm^{-1} [4,32]. The O–H bend is sharp for both ZnO-FS and ZnO-DS but broad

for ZnO-FH. This is because ZnO-FH was synthesized from leaves with heating as the method of extraction, and heating is known to cause broadening of IR peaks [35]. Furthermore, both ZnO-FS and ZnO-DS possessed another peak at ~870 cm^{-1} attributed to Zn–OH, but this peak was absent in ZnO-FH. It has been reported that heating tremendously decreased the intensity of the peak attributed to the degradation of hydroxyl groups in hemicelluloses [36]. Thus, it can be assumed that heating breaks the Zn–OH bond in ZnO-FH. The different functional groups present in the synthesized nanoparticles proved the attachment of phytochemicals from *A. squamosa* leaves on the surface of the ZnO NPs. These phytochemicals may be responsible for the formation of ZnO NPs by reducing zinc nitrate to zinc oxide. Moreover, it is also predicted to play an important role in the stabilization of the biosynthesized nanoparticles by acting as a capping agent [34]. They also influence the formation of the synthesized ZnO NPs, such as in their development and the onset of crystal formation. Figure 4 shows SEM images of ZnO-FH, ZnO-FS, and ZnO-DS at a magnification power of 25,000 with calculated average particle sizes of 111 nm, 88 nm, and 68 nm, respectively. The particle size distribution graphs are displayed in Figure S1. It can be observed that using dehydrated leaves for ZnO synthesis resulted in a smaller average particle size than using fresh leaves. The SEM images of ZnO-FH and ZnO-FS show homogeneous, agglomerated, and almost spherical particles, while ZnO-DS surface morphology resembles a coral-like structure surrounded by a cluster of spherical particles. The agglomeration observed in all solids shows large spaces between particles, forming pores, which could result from gas escaping at high pressure during combustion. The morphology of the solids reflects the method of preparing the extract that significantly influences their growth, surface morphology, and size.

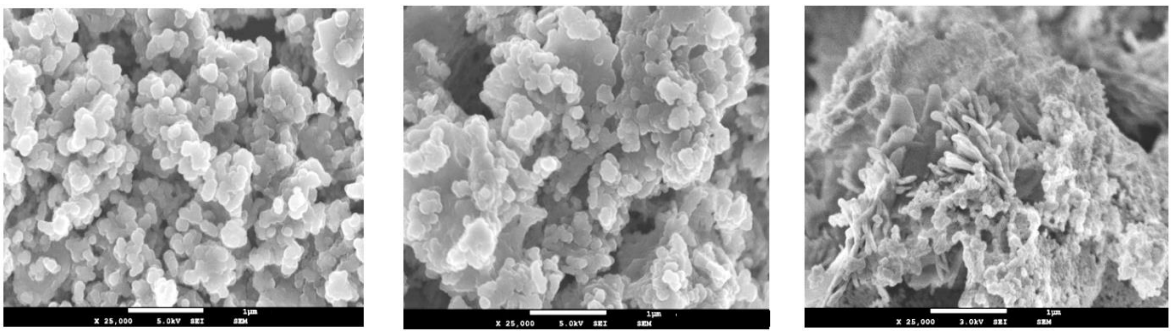

(a) **(b)** **(c)**

Figure 4. SEM images of leaf extracts **(a)** LE-FH; **(b)** LE-FS; **(c)** LE-DS at x25,000 magnification.

Figure 5 exhibits the diffraction patterns obtained for all synthesized ZnO NPs. The diffraction peaks of each of the synthesized nanomaterials observed at 2θ (in degrees) are 32.23°, 34.93°, 36.71°, 48.02°, 57.09°, 63.26°, and 68.40° corresponding to (100), (002), (101), (102), (110), (103), (200) and (112) planes, respectively. Each X-ray diffractogram shows well-defined peaks that matched with a hexagonal wurtzite phase according to the standard pattern of JCPD ZnO 00-075-0576. Debye-Scherrer equation and Bragg's equation were used to calculate the average crystallite size and the d-spacing of all the synthesized ZnO NPs, respectively. Table 2 shows 2θ and d-spacing values for the three most intense peaks at (100), (002), and (101), and Table 3 shows the calculated lattice parameters a and c, the average crystallite size, and the unit cell volume, V(Å)^3, for all the samples. The average crystallite size of the three synthesized ZnO ranges from 11.03 to 11.29 nm. The broad diffraction peaks in the XRD pattern clearly indicate that small nanocrystals are present in the samples. Extra peak attributed to (001) at 2θ value of 29.85° is believed to be due to its lattice strain and interplanar

spacing [37]. Table S1 shows the XRD peak lists for ZnO-FS (a), ZnO-DS (b), and ZnO-FH (c).

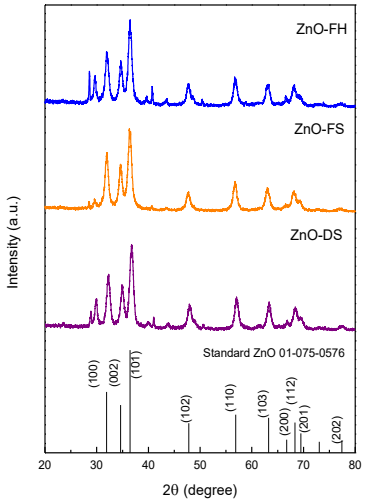

Figure 5. XRD patterns of standard ZnO, LE-FH, LE-FS, and LE-DS.

Table 2. Values of the diffraction angle 2θ in degrees (°) and d-spacing (Å) for the three most intense peaks.

Samples	(100)		(002)		(101)	
	2θ (°)	d-spacing (Å)	2θ (°)	d-spacing (Å)	2θ (°)	d-spacing (Å)
ZnO-FH	32.0157	2.77491	34.9302	2.56659	36.7189	2.44557
ZnO-FS	31.9131	2.80202	34.5926	2.59087	36.3871	2.46710
ZnO-DS	31.9703	2.79714	34.6641	2.58569	36.4328	2.46411

Table 3. Structural lattice parameters, α and c (Å), average crystallite size (nm), and unit cell volumes $(Å)^3$ obtained from XRD patterns of ZnO NPs synthesized.

Samples	Lattice parameters		Average crystallite size (nm)	Unit cell volume $V(Å)^3$
	a (Å)	*c* (Å)		
ZnO-FH	3.21	5.18	11.03	46.12
ZnO-FS	3.23	5.19	11.29	47.09
ZnO-DS	3.23	5.18	11.18	46.83

3.2. Phytochemical screening.

Phytochemical assays of plant extracts and their green-synthesized nanoparticles are vital, as they reveal the bioactive components present, which can be useful in the manufacture of effective drugs [38]. Owing to their multiple biological properties, flavonoids and phenolic compounds are deemed to be the more prominent phytochemicals [39]. The qualitative phytochemical analysis of the *A. squamosa* leaf extracts and the synthesized phytogenic ZnO NPs using water as a solvent is shown in Table 4. The assay revealed the presence of flavonoids, phenols, tannins, and glycosides in the leaf extracts.

The phytochemicals present in the leaf extracts of *A. squamosa* in water were discovered to be flavonoids, phenols, glycosides, oils, and saponins by Simon *et al*. [40]. However, phenols were absent when acetone was used as the solvent, and both phenols and flavonoids were absent with chloroform as the solvent [40]. In another article, phytochemicals were extracted using the Soxhlet method, and methanol was shown to extract more phytochemicals, including volatile oils, alkaloids, flavonoids, polyphenols, glycosides, carbohydrates, saponins, and tannins [41]. The differences in the phytochemicals detected in this study may be due to genetic, variety, and regional variations in *A. squamosa*, different solvents used, and different extraction methods. However, the assay showed that none of the aforementioned phytochemicals were detected in the green-synthesized ZnO NPs. This observation is in contrast with the IR analyses obtained for the ZnO samples (section 3.1).

According to the IR spectra of all samples, functional groups of organic molecules present in the leaf extracts were also found in the biosynthesized ZnO NPs. This could mean that the phytochemicals strongly adhered to the surface of the ZnO NPs and did not dissolve in the aqueous medium.

Table 4. Phytochemical screening of the leaf extracts and the biosynthesized ZnO NPs.

Sample / Phytochemical	ZnO-FH	LE-FH	ZnO-FS	LE-FS	ZnO-DS	LE-DS
Alkaloids	-	-	-	-	-	-
Quinones	-	-	-	-	-	-
Saponins	-	-	-	-	-	-
Flavonoids	-	+	-	+	-	+
Phenols	-	+	-	+	-	+
Tannins	-	+	-	+	-	+
Glycosides	-	+	-	+	-	+
Cardiac glycosides	-	-	-	-	-	-

ey: (+): Present; (-): Absent; ZnO-FH: ZnO from fresh leaves (heat); LE-FH: Fresh leaves (heat); ZnO-FS: ZnO from fresh leaves (sonicate); LE-FS: Fresh leaves (sonicate); ZnO-DS: ZnO from dried leaves (sonicate); LE-DS: Dried leaves (sonicate).

3.3. Total phenolic contents (TPC).

The total phenolic content (TPC) of the leaf extracts was determined using the Folin-Ciocalteu reagent (FCR), and the TPC values were calculated from the equation of the standard gallic acid calibration, $y = 0.0087x + 0.0793$, $R^2 = 0.9939$. The analyses were repeated three times, and the TPC values were reported as the average on a gallic acid equivalent basis. From the experiment, it was observed that as the concentration of gallic acid in the sample increases, the solution's blue color intensity increases.

From the TPC results shown in Figure 6, phenolics, which are the fundamental natural antioxidants, were found to be present in large amounts in all the leaf extract samples. The presence of this phytochemical can also be verified by the color change of the sample solutions from colorless to blue. The blue color is caused by the reduction of FCR by phenolics [42]. 1000 ppm of leaf extracts synthesized from dried leaves (LE-DS) had the highest phenolic content (150.35 ± 4.25 mg GAE/g crude extract), followed by those synthesized from fresh leaves, 129.66 ± 0.33 and 122.34 ± 2.06 mg GAE/g crude extract for LE-FH and LE-FS, respectively. Al-Nemari *et al.*[43] reported the TPC value of 80 ppm dried leaves powder of *A. squamosa* using three different solvents: methanol, acetone, and water. Interestingly, the highest TPC value (282.1 mg GAE/g) was obtained when methanol was used as the extraction solvent, and the lowest TPC value (16.9 mg GAE/g) was reported when extracted using water.

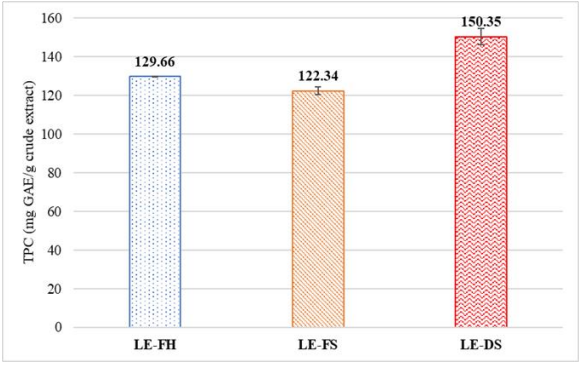

Figure 6. TPC values for the leaf extracts.

Between the fresh and dried leaf extracts, the dried leaf extracts (LE-DS) were discovered to possess the highest phenolic content (150.35 ± 4.25 mg GAE/g crude extract). Our results corroborated those findings as reported by Wanyo and co-workers, stating that high phenolics (51 mg GAE/g dry sample) were evaluated from aqueous extract dried mulberry leaves than the fresh ones [44]. It was deduced that the presence of heat during sample drying may lead to the degradation of phenolic compounds, releasing antioxidants. By comparing the TPC values of *A. squamosa* and mulberry leaves, it can be presumed that *A. squamosa* is a better antioxidant than mulberry, owing to its higher value. In another study reported by Najafabad *et al*[45], dried plum extracts had a higher phenolic content compared to the fresh ones. It was found that the higher antioxidant activity may be due to the presence of only a small amount of moisture in the dried plum extracts, which can promote lipid oxidation and lead to the production of free radicals. In addition, Uribe *et al*. [46] revealed high phenolic content in dried peppermint leaves when compared to fresh ones. This is because drying can damage the leaves' texture by softening the matrix and disrupting the cell membrane, releasing phenolic compounds. Therefore, a higher TPC value for the dried leaf extracts of *A. squamosa* was expected when compared to the fresh leaf extracts.

For the *A. squamosa* fresh leaf extracts, the TPC value was 129.66 ± 0.33 mg GAE/g crude extract at 60°C (LE-FH), but it was only 122.34 ± 2.06 mg GAE/g crude extract at room temperature (LE-FS). The heating process could have caused the production of more phenolics than the sonication method at room temperature. High temperatures can disrupt the cell walls of plant tissue, reducing interactions between phenols and proteins or polysaccharides. As a result, more polyphenols diffuse into the solvent, increasing the amount of flavonoids, since flavonoids are commonly found as glycosides. A higher temperature can also speed up the rate of solubility of phenolic compounds and their rate of diffusion, increasing the phenolic content [47]. However, heating beyond certain temperatures during sample extraction may decompose and deteriorate phenolic and flavonoid residues. In addition, high temperatures promote solvent loss, in which evaporation of phytochemicals may occur, reducing the phenolic and flavonoid content [48]. For instance, Ma *et al*. [49] demonstrated that increasing the temperature from 15°C to 30°C during the extraction of citrus peel increased the yield of phenolic acids, indicating higher antioxidant activity. However, temperatures above 50°C lowered the stability of phenolic compounds. Therefore, it is vital to choose an optimal temperature for sample extraction, as higher temperatures may cause phytochemicals to evaporate or degrade. On the other hand, lower temperatures may provide insufficient heat for the extraction of the natural antioxidants present in plant samples.

3.4. Total flavonoid content (TFC).

The total flavonoid content (TFC) was carried out via the colorimetric aluminum chloride method, and the TFC values were calculated from the equation of the quercetin standard curve, $y = 0.0074x - 0.0022$, $R^2 = 0.9992$. The test was repeated three times, and the TFC values were expressed as the average in terms of quercetin equivalents. The yellow color intensity of the solution also increases with an increase in the concentration of quercetin.

From the TFC results shown in Figure 7, all leaf extract samples possessed low secondary metabolites such as flavonoids (~20 mg QE/g crude extract). The presence of this phytochemical can also be proven by the color change of the sample solutions from colorless to yellow. The yellow color is caused by the complexation of Al(III) with the 3-hydroxy – 4-carbonyl groups (3,4-site) in flavonoid [50].

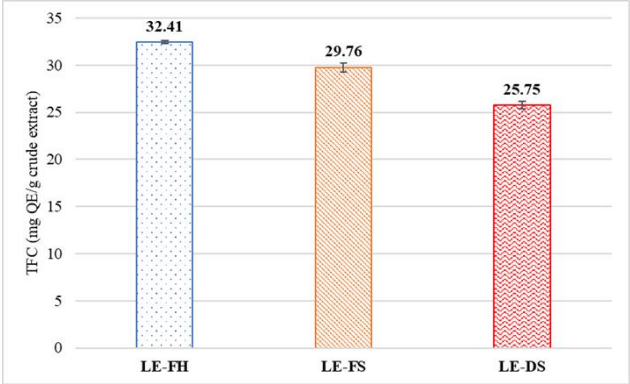

Figure 7. TFC values for the leaf extracts.

Al-Nemari *et al*. [43] reported TFC values of 0.1 mg QE/g when 80 ppm of dried leaves powder of *A. squamosa* were extracted using water. A higher flavonoid content (25.75 mg QE/g) was detected in this study using 1000 ppm of aqueous extract of dried leaf powder. In this study, fresh leaf extracts with heating as the method of extraction (LE-FH) had the highest flavonoid content (32.41 ± 0.16 mg QE/g crude extract). Similar findings were observed where high flavonoids (24.33 mg RE/g dry sample) were reported using the aqueous extract of mulberry fresh leaves [44]. Higher temperatures can increase phytochemical evaporation by reducing solvent content, thereby decreasing the concentration of phenolics and flavonoids [48]. Hence, it can be inferred that dried leaves may contribute to the loss of phytoconstituents, leading to higher TFC values in the fresh samples.

Similar to the TPC assay, heating also produced slightly more flavonoids than sonicating at room temperature. For instance, the TFC value of LE-FH was 32.41 mg QE/g crude extract at 60°C, but only 29.76 mg QE/g crude extract for LE-FS at room temperature. A synonymous result can be seen in the flavonoid assay of heat-treated *Gynura divaricata* leaf extracts at different temperatures. At 100°C, the TFC value was 47.52 mg Kaempferol/g dry material, which was higher than the value at 40°C, i.e., 19.16 mg Kaempferol/g dry material. The mechanism was that a higher extraction temperature increased the diffusion coefficients and solubility of polyphenol. In addition, the discharge of bound polyphenols reduced their coagulation with lipoprotein and thus, increased the concentration of free polyphenols [51].

The experimental results for all ZnO samples show that phenolic compounds were not detected, and only a very small concentration of flavonoids (~1 mg QE/g crude extract) was detected. The solutions remained colorless in both tests, indicating that the levels of phenolics and flavonoids were too low. However, *Peganum harmala* mediated ZnO NPs using zinc acetate as the precursor had a slightly higher TPC and TFC values (9.31 and 10.85) than its crude extract (8.22 and 10.44) [52]. The type of precursor plays an important role in the size of nanoparticles. ZnO synthesized from zinc acetate had a smaller size compared to that synthesized from zinc nitrate [53]. In this experiment, zinc nitrate was used as the precursor, which may result in larger ZnO particles being synthesized, giving a smaller surface area-to-volume ratio for capping phenolics and flavonoids from *A. squamosa* leaves. Furthermore, the type of solvent used plays an important role in extracting secondary metabolites. Studies have shown that the methanol extract yields a higher quantity of phytochemicals from plants than other solvents, such as water, chloroform, ethyl acetate, and petroleum ether. This is because methanol can dissolve both polar and non-polar bioactive compounds due to its intermediate polarity [54]. Since water was used as the solvent in this experiment, fewer phytochemicals

may be extracted from the plant, potentially resulting in lower adherence of phenolics and flavonoids to the surface of the synthesized ZnO NPs.

3.5. DPPH assay.

Human metabolism leads to the production of free radicals. However, oxidative stress can cause an overproduction of free radicals that contribute to many diseases such as heart disease, Parkinson's, Alzheimer's, cancer, and many more. Therefore, humans require antioxidants that can prevent the occurrence of such diseases by scavenging free radicals. Plants can act as free radical scavengers as they are rich in phenolic constituents such as phenolic acids and flavonoids, which have hydrogen-donating properties [55]. The free radical scavenging assay is established on the ability of antioxidants to donate an electron or proton to the free radical N atom in DPPH. Scavenging free radicals results in a color change from purple DPPH to yellow DPPH, accompanied by a decrease in absorbance. The percentage of inhibition of DPPH free radical increases with antioxidants. In addition, IC_{50} values are commonly calculated to determine the antioxidant capacity of a sample. The lower the IC_{50} value, the higher the antioxidant potential. This means that only a low concentration of antioxidant molecules is required to inhibit 50% of free radicals [56]. In this study, the DPPH assay was carried out at various concentrations for the leaf extracts (0.1 – 0.5 mg/mL) and ZnO NPs (2 – 10 mg/mL). It was observed that the % inhibition of DPPH free radical increases with an increase in the concentrations of both leaf extracts (Figure S2) and the biosynthesized ZnO NPs.

Among the three types of leaf extract samples, the dried leaves (LE-DS) were found to be the most promising free radical scavenger with the lowest IC_{50} value of 295 ppm (Table 5). The low IC_{50} value was contributed to by a high phenolic content (Figure 6). In addition, the presence of flavonoids, tannins, and glycosides observed in Table 4 may also be able to scavenge the free radicals. The IC_{50} value for DPPH scavenging activity for LE-FH and LE-FS was 357 ppm and 314 ppm, respectively. However, all of the *A. squamosa* leaf extracts have lower antioxidant activity when compared to standard ascorbic acid (6.67 ppm). From the phytochemical analysis in this experiment, the leaves of *A. squamosa* contain phenols, flavonoids, tannins, and glycosides that act as natural antioxidants. Longer hours of extraction can lead to more phytochemicals being extracted. For instance, long maceration hours (48 hours) of *A. squamosa* leaves in distilled water produced a high antioxidant activity with an IC_{50} value of 98.3 ppm [43].

Table 5. IC_{50} values and DPPH radical inhibition activity (%) of samples.

Sample	IC_{50} (ppm)	DPPH inhibition activity (%)
Ascorbic acid	6.67	
LE-FH	357	13.27
LE-FS	314	16.29
LE-DS	295	20.57

The presence of bioactive phytochemicals, such as phenolics and flavonoids, confers redox properties, enabling them to donate hydrogen atoms [57]. In the current study, the dried sample (LE-DS) had the highest % inhibition among the fresh samples (LE-FH and LE-FS). At 0.1 ppm, the radical scavenging activity (RSA) for LE-FH, LE-FS, and LE-DS was 13.27%, 16.29%, and 20.57%, respectively. Our results were in agreement with a previously reported paper on fresh and vacuum-oven-dried *Cayratia trifolia* leaves. The dried leaves had 88.41%

of radical scavenging activity, whereas the fresh leaves only had 41.40% [58]. The drying of plant samples weakens the plant tissue, leading to cell wall disintegration during extraction. This, in turn, leads to greater release of phenolics and flavonoids from the leaves. On the contrary, the degradation of antioxidant components by enzymes may occur in fresh samples, as enzymes remain active, reducing the concentrations of phenolics and flavonoids [59]. The degree of DPPH radical inhibition also depends on the number of hydroxyl groups. Gallic acid exhibited a high radical scavenging activity owing to numerous hydroxyl-substituted groups [60]. Thus, the high DPPH inhibition activity of ascorbic acid in this experiment may be due to the presence of four hydroxyl groups. La *et al*. [61] explained that the difference in DPPH radical inhibition is affected by the position of the bulky phenolics, the polarity of the solvent, and hydrogen bond formation between the antioxidant molecule and solvent. Although phenols were qualitatively detected during phytochemical screening, the extracted phenolics may have bulky structures that can hinder their radical-scavenging activity. An increase in antioxidant activity can be achieved if the bulky hydrophilic group of phenol is far away from the hydroxyl group. Besides, the formation of hydrogen bonds between the antioxidant molecule and the solvent increases the likelihood of interaction between the antioxidant and DPPH. In this experiment, DPPH was dissolved in methanol. This means that the phenols present in the leaf extracts can form hydrogen bonds with methanol and thus interact with DPPH. Depending on the type of solvent used, antioxidants can react with DPPH radical via two mechanisms: electron transfer or hydrogen atom transfer. Electron donation from the antioxidant molecule to the DPPH radical is the main pathway in alcoholic solvents, whereas hydrogen atom donation is the major mechanism in non-polar solvents [61]. Figure 8 illustrates the reaction mechanism for phenolics acting as a free radical scavenger by donating one of its hydrogen atoms to the nitrogen free radical in DPPH. This results in the neutralization of free radicals and the formation of a stable product.

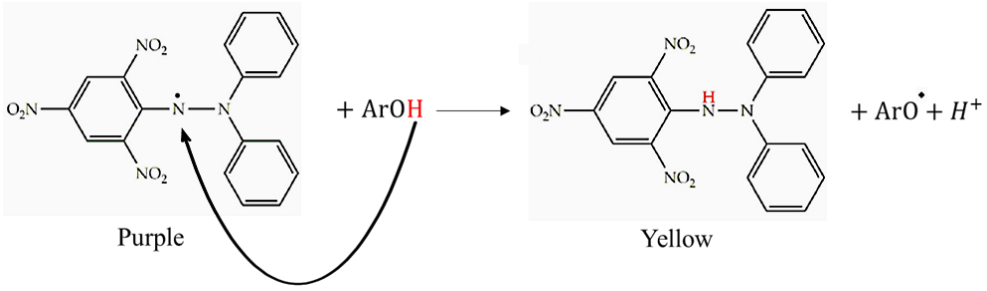

Figure 8. DPPH reaction mechanism via hydrogen atom transfer.

The antioxidant activity of all of the synthesized ZnO samples was also investigated. The radical inhibition activity increased with an increase in the concentration of green-synthesized ZnO NPs. (Figure 9) However, very low activity was observed in ZnO-FH. The activity was only 2.86% at 10 mg/mL. This was then followed by ZnO-FS, in which the activity was 15.31% at the same concentration. Furthermore, the increase in activity was small in both ZnO-FH and ZnO-FS. ZnO-DS was the best DPPH radical scavenger with an RSA of 20.25% at 10 mg/mL. There was also a larger increase in activity as compared with ZnO-FH and ZnO-FS. SEM analysis showed agglomeratioin the three synthesized ZnO samples, which could reduce the number of available active sites for reactions, limiting antioxidant activity compared to the leaf extract. ZnO-DS exhibits better activity, which could be attributed to its surface morphology resembling a coral-like structure with more porous morphology [62].

Additionally, the average particle size of ZnO-DS is smaller compared to ZnO-FH and ZnO-FS, further enhancing its performance.

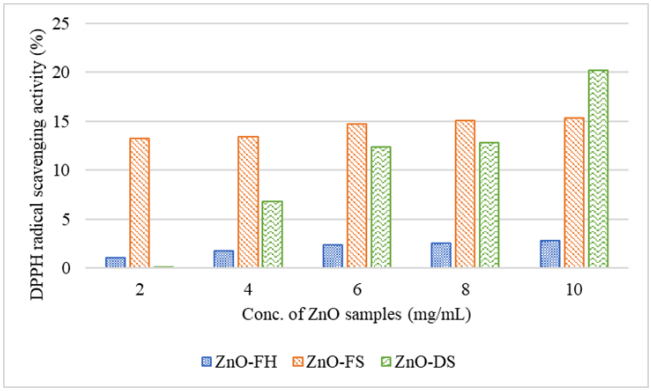

Figure 9. Inhibition of DPPH free radical (%) by 2 – 10 mg/mL of ZnO NPs.

The current study concluded that the DPPH radical scavenging assay of ZnO NPs synthesized from *A. squamosa* was lower than that of the leaf extracts. Similar observations were reported by Shabaani, who found that the inhibition activity of ZnO NPs synthesized from loquat (Eriobotry*a japonica*) seed extract was lower than that of the seed extract [63]. This may be due to insufficient capping of bioactive phytochemicals from the seed extract onto the surface of the ZnO NPs, resulting in an inadequate concentration of phytochemicals required for a desirable antioxidative property. Furthermore, studies have shown that some plant extracts, such as *Myrica esculenta* and *Garcinia cambogia*, exhibited higher antioxidant activity than their corresponding ZnO NPs. This was contributed by bioactive phytochemicals, such as phenolics and flavonoids, which also play a vital role as capping and reducing agents in the synthesis of nanoparticles [64,65].

3.6. FRAP assay.

The FRAP assay is based on the ability of antioxidants to reduce potassium ferricyanide (Fe^{3+}) to potassium ferrocyanide (Fe^{2+}), followed by the reaction with ferric chloride to produce a ferric-ferrous complex that absorbs at 700 nm [66]. Antioxidants reduce Fe^{3+} to Fe^{2+} by electron donation, causing a color change from yellow to various shades of blue or green [67]. The increase in reducing power is characterized by an increase in absorbance [68]. FRAP values were derived from the equation of the ferrous sulfate standard curve, $y = 0.0003x + 0.0489$, $R^2 = 0.9836$. The FRAP assay was conducted using a constant concentration of 100 ppm for both the leaf extracts and ZnO NPs.

The FRAP experimental data of leaf extracts (Figure 10) demonstrated that all leaf extract samples possessed ferric ion-reducing properties. A similar trend was observed in the FRAP assay, in which dried leaves showed stronger reducing power than fresh leaves. However, FRAP values obtained were low (5.6 – 6.7 mg FSE/g crude extract). Both types of fresh leaf extracts (LE-FH and LE-FS) exhibited almost similar and lower strength of reducing power (5.59 ± 0.07 and 6.22 ± 0.07 mg FSE/g crude extract). Meanwhile, the dried leaf extracts (LE-DS) had the highest FRAP value of 6.70 ± 0.09 mg FSE /g crude extract. As expected, pure ascorbic acid was used as a standard in this study, giving a higher FRAP value of 59.17 ± 0.71 mg FSE/g crude extract when compared to our leaf extracts.

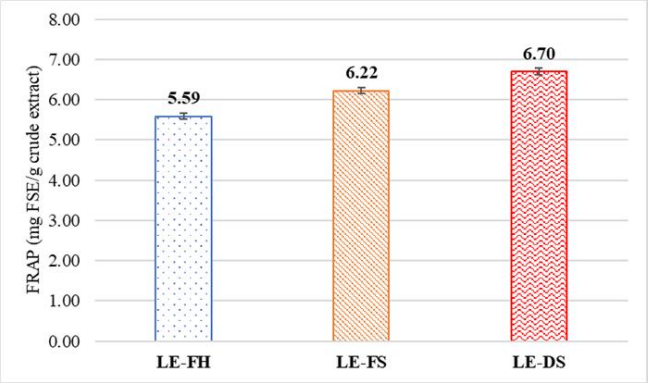

Figure 10. FRAP value of leaf extract samples.

An identical trend was observed between the FRAP and DPPH assays. However, the lower FRAP values might be due to the FRAP mechanism being based on electron transfer rather than hydrogen-atom transfer [69]. Figure 11 demonstrates the reducing power of organic molecules such as phenolics and flavonoids by donating an electron to reduce Fe^{3+} to Fe^{2+}. The current findings agree with the literature, which ascribes the reducing power of A. squamosa leaf extracts to its ability to transfer electrons in a redox reaction, and the reducing strength is weaker than that of ascorbic acid [70]. The capability of the plant extracts in the reduction of Fe^{3+} may be associated with the hydrogen-donating effect of phenolics. Phenolics are known to be the major contributors to an antioxidant, and the antioxidant activity is dependent on the concentration of phenolics [71]. Hence, the high antioxidant activity of the leaf extracts may be attributed to the presence of phenols and flavonoids, as detected by FTIR analysis and phytochemical screening.

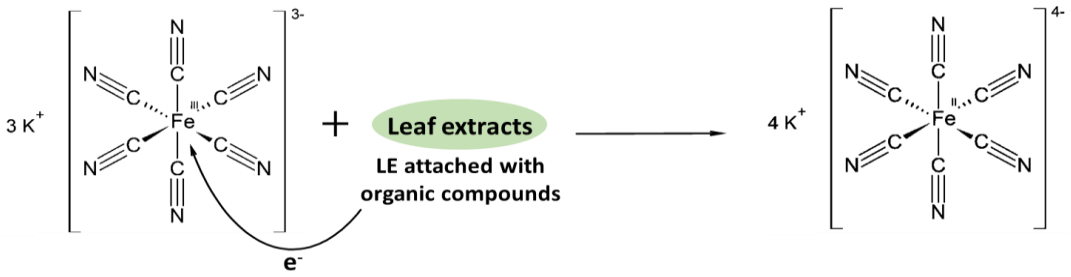

Figure 11. FRAP reaction mechanism via electron transfer.

Among the fresh and dried leaves, the *A. squamosa* dried leaves (LE-DS) exhibited the highest FRAP value. Similar findings were observed by Kozlowska *et al.*[72], where dried Indian borage leaves had a higher FRAP value than the fresh ones. Drying the sample is a factor that can alter the amount of bioactive molecules responsible for the antioxidant potential in plants. It was concluded that drying did not cause any loss of phenolic compounds, which may reduce the antioxidant activity of the extracts. Instead, it strengthened the antioxidant property. Initial removal of water from plant samples will soften the plant matrix and degrade the cell wall, leading to greater diffusion of phenolics and flavonoids onto the leaf surface [59].

The ferric ion-reducing ability of the *A. squamosa* fabricated ZnO NPs was not detected. In a study by Pulido *et al.* [73] on the ferric ion-reducing activity of polyphenols in water and methanol, they found that absorbance continued to increase even after a few hours of reaction time. Thus, it can be deduced that not all phenolics capped onto the surface of ZnO NPs can reduce Fe^{3+} at a fast rate as predicted. In addition, the coating of phytochemicals on

the surface of the synthesized nanomaterials may be insufficient, preventing them from reducing Fe^{3+} to Fe^{2+}.

3.7. α-glucosidase activity.

Diabetes mellitus (DM) is defined as a state of hyperglycemia in either fasting or postprandial states. Diabetes is categorized into two types: Type 1 and Type 2. Type 1 DM is related to insulin deficiency, whereas type 2 DM is established on insulin resistance, and it is the more common type [74]. α-glucosidase is an enzyme that catalyzes the hydrolysis of starch in the intestine [75]. There are commercially available α-glucosidase inhibitors, including acarbose, miglitol, and voglibose, that can decrease postprandial hyperglycemia by slowing the rate of carbohydrate digestion in the small intestine [76]. However, these enzyme inhibitors can cause unwanted gastrointestinal adverse effects, making them undesirable as antidiabetic agents [75]. Thus, researchers are now focusing on plant extracts, which are less toxic and have minimal negative effects, as an alternative source of therapeutic agents [77].

The α-glucosidase inhibition activity (%) of *A. squamosa* leaf extracts and ZnO NPs was evaluated using 100 ppm for each sample. As shown in Figure 12, both leaf extracts and green-synthesized ZnO NPs exhibited α-glucosidase inhibition activity, with the leaf extracts demonstrating greater antidiabetic activity than the nanoparticles. However, the antidiabetic property was weak for all samples. Among the leaf extracts, fresh leaf extracts (LE-FH and LE-FS) had a lower activity than the dried leaf extracts (LE-DS). The α-glucosidase inhibition activity for LE-FS, LE-FH, and LE-DS is 7.31%, 10.83%, and 10.93%, respectively. In the synthesized ZnO NPs, the same trend was observed as in the leaf extracts, in which nanoparticles synthesized from dried leaves (ZnO-DS) displayed stronger enzyme inhibition activity compared to those synthesized from fresh leaves (ZnO-FH and ZnO FS). The enzyme inhibition activity for ZnO-FS, ZnO-FH, and ZnO-DS is 2.67%, 6.85%, and 7.68%, respectively. As predicted, pure acarbose was used as a standard in the current study, yielding the highest inhibition activity of 98.78% compared with our samples.

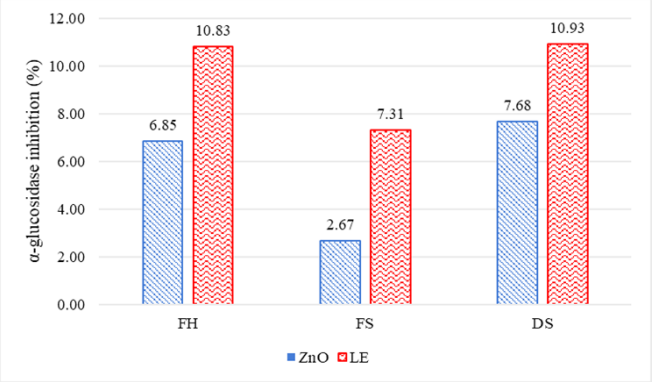

Figure 12. α-glucosidase inhibition of 100 ppm of leaf extracts and ZnO NPs.

In a study by Ranjana and Tripathi [78], tissue homogenate from the intestine of normal rats was used as an enzyme source to determine the α-glucosidase inhibition activity of hexane, methanol, and water extracts of *A. squamosa* leaves. The experimental data showed that the hexane extract had the highest inhibition compared to the water and methanol extracts. This could be attributed to the presence of a higher concentration of non-polar phytochemicals. The mechanism of enzyme inhibition was thought to be the ability of phytochemicals to stimulate insulin secretion and increase insulin levels. Moreover, polyphenolic compounds can inhibit

the activity of α-glucosidase by binding to it [78]. The inhibitory activity of α-amylase and α-glucosidase in plant extracts from the Brazilian Cerrado was also contributed to by phenolics, particularly flavonoids and tannins. Tannin can act as an enzyme inhibitor by binding to the active or secondary sites of the enzyme, forming enzyme-inhibitor complexes [79]. Tannin was also found to be a non-competitive inhibitor by binding to a non-active site of α-amylase and α-glucosidase in *Azadirachta indica* leaf extracts [80]. This could be the mechanism of action of *A. squamosa* leaf extracts and ZnO NPs in this experiment, as they contain flavonoids and tannins, which were detected during phytochemical screening and FTIR analysis. However, the weak enzyme-inhibition activity may be due to the low levels of flavonoids and tannins present.

4. Conclusion

In this work, a cost-effective, environmentally friendly, and simple green synthesis of ZnO NPs was successfully achieved using aqueous extracts of fresh and dried *Annona squamosa* Linn leaves. Phenolics were found in high amounts, with the dried leaf extracts (LE-DS) showing the highest TPC value of 150.35 ± 4.25 mg GAE/g crude extract. Flavonoids were present in smaller quantities, with the fresh leaf extract (LE-FH) exhibiting the highest TFC value of 32.41 ± 0.16 mg QE/g crude extract. In the DPPH assay, LE-DS demonstrated the strongest radical scavenging activity, with the lowest IC_{50} value of 295 ppm. Furthermore, LE-DS exhibited the strongest ferric ion reducing power with a FRAP value of 6.70 ± 0.09 mg FSE /g crude extract compared to LE-FH and LE-FS. FTIR spectroscopy revealed the presence of phytochemicals such as phenols, flavonoids, and proteins in the leaf extracts. The analysis further confirmed the successful synthesis of ZnO NPs from leaf extracts, as evidenced by the presence of Zn-O and Zn-OH bands. Organic functional groups from the phytochemicals in the extracts were also detected in the nanoparticles, indicating their role in stabilizing and capping ZnO NPs. Qualitative phytochemical screening revealed that the *A. squamosa* leaf extracts contained flavonoids, phenols, tannins, and glycosides. No phytochemicals were detected in the ZnO NPs, likely due to their insolubility in aqueous media and the strong adherence of metabolites to the nanoparticle surface. In the DPPH assay, ZnO NPs exhibited concentration-dependent free radical scavenging, with ZnO NPs synthesized from dried leaves (ZnO-DS) showing the highest radical scavenging activity of 20.25%. Both leaf extracts and ZnO NPs inhibited α-glucosidase, albeit with relatively low activity. Overall, the dried leaf extracts of *A. squamosa* demonstrated enhanced antioxidant and antidiabetic activities compared to the fresh leaf extract. These findings suggest that *A. squamosa* dried leaves could serve as a valuable source for the synthesis of bioactive extracts and ZnO NPs. However, further *in vivo* and mechanistic studies are needed to confirm their biological efficacy, safety, and potential applications. Future research should also explore optimal synthesis parameters and possible synergistic effects with other bioactive compounds, highlighting the dried leaves as a versatile source for multifunctional applications.

Author Contributions

Conceptualization – A.L.T., H.M.Y., X.X., Y.Y.; Methodology – A.L.T., H.M.Y., S.M.S.C.; Validation – A.L.T., H.M.Y., S.M.S.C.; Formal analysis – A.L.T., H.M.Y., S.M.S.C.; Investigation – A.L.T., H.M.Y., S.M.S.C.; Resources – A.L.T., H.M.Y., S.M.S.C.; Data curation – X.X.; Writing – original draft preparation – A.L.T., H.M.Y., S.M.S.C.; Writing –

review & editing – A.L.T., H.M.Y., S.M.S.C.; Visualization – A.L.T., H.M.Y.; Supervision – A.L.T., H.M.Y.; Project administration – A.L.T., H.M.Y.; Funding acquisition – A.L.T., H.M.Y. All authors have read and agreed to the published version of the manuscript.

Institutional Review Board Statement

Not applicable.

Data Availability Statement

Data supporting the findings of this study are available upon reasonable request from the corresponding author.

Funding

This work is supported by Universiti Brunei Darussalam Research grant UBD/RSCH/1.4/FICBF/2024/075.

Acknowledgments

The authors would like to acknowledge Universiti Brunei Darussalam for extending their facilities for all analyses (FTIR, XRD, UV-Vis, and SEM). We want to thank Nur Shaidatul Najihah binti Matussin for preparing the XRD tables.

Conflicts of Interest

Authors declare no conflict of interest.

References

1. Jamkhande, P.G.; Ghule, N.W.; Bamer, A.H.; Kalaskar, M.G. Metal nanoparticles synthesis: An overview on methods of preparation, advantages and disadvantages, and applications. *J. Drug Deliv. Sci. Technol.* **2019**, *53*, 101174, https://doi.org/10.1016/j.jddst.2019.101174.
2. Singh, T.A.; Sharma, A.; Tejwan, N.; Ghosh, N.; Das, J.; Sil, P.C. A state of the art review on the synthesis, antibacterial, antioxidant, antidiabetic and tissue regeneration activities of zinc oxide nanoparticles. *Adv. Colloid Interface Sci.* **2021**, *295*, 102495, https://doi.org/10.1016/j.cis.2021.102495.
3. Mishra, P. K.; Mishra, H.; Ekielski, A.; Talegaonkar, S.; Vaidya, B. Zinc oxide nanoparticles: a promising nanomaterial for biomedical applications. *Drug Discov Today* **2017**, *22*, 1825–1834, https://doi.org/10.1016/j.drudis.2017.08.006.
4. Rahman, A.; Tan, A.L.; Harunsani, M.H.; Ahmad, N.; Hojamberdiev, M.; Khan, M.M. Visible light induced antibacterial and antioxidant studies of ZnO and Cu-doped ZnO fabricated using aqueous leaf extract of Ziziphus mauritiana Lam. *J. Environ. Chem. Eng.* **2021**, *9*, 105481, https://doi.org/10.1016/j.jece.2021.105481.
5. Martínez-Chávez, L.A.; Hernández-Ramírez, M.Y.; Feregrino-Pérez, A.A.; Esquivel Escalante, K. Cutting-Edge Strategies to Enhance Bioactive Compound Production in Plants: Potential Value of Integration of Elicitation, Metabolic Engineering, and Green Nanotechnology. *Agronomy* **2024**, *14*, 2822, https://doi.org/10.3390/agronomy14122822.
6. Azeem, M.; Siddique, M.H.; Imran, M.; Zubair, M.; Mumtaz, R.; Younas, M.; Abdel-Maksoud, M.A.; El-Tayeb, M.A.; Rizwan, M.; Yong, J.W.H. Assessing anticancer, antidiabetic, and antioxidant capacities in green-synthesized zinc oxide nanoparticles and solvent-based plant extracts. *Heliyon* **2024**, *10*, e34073, https://doi.org/10.1016/j.heliyon.2024.e34073.
7. Rani, S.; Gahlot, K.; Kumar, A. Experimental evidences of antidiabetic activity of aqueous extract of Cressa cretica L. on streptozotocin induced diabetes in rats. *Lett. Appl. NanoBioSci.* **2020**, *9*, 774–778, https://doi.org/10.33263/LIANBS91.774778.

8. Motelica, L.; Vasile, B.-S.; Ficai, A.; Surdu, A.-V.; Ficai, D.; Oprea, O.-C.; Andronescu, E.; Mustățea, G.; Ungureanu, E. L.; Dobre, A.A. Antibacterial Activity of Zinc Oxide Nanoparticles Loaded with Essential Oils. *Pharmaceutics* **2023**, *15*, 2470, https://doi.org/10.3390/pharmaceutics15102470.
9. Al-Harthi, H. F.; Baker, A.; Elgorban, A. M.; Bahkali, A. H.; Shaikh, A. M.; Kovács, B.; Khan, M. S.; Syed, A. Novel Bioengineered Antibacterial and Anticancer ZnO Nanoparticles. *J. Biomed. Nanotechnol.* **2022**, *18*, 1106–1120, https://doi.org/10.1166/jbn.2022.3308.
10. Rehana, D.; Mahendiran, D.; Kumar, R.S.; Rahiman, A.K. In vitro antioxidant and antidiabetic activities of zinc oxide nanoparticles synthesized using different plant extracts. *Bioprocess Biosyst. Eng.* **2017**, *40*, 943–957, https://doi.org/10.1007/s00449-017-1758-2.
11. Velsankar, K.; Venkatesan, A.; Muthumari, P.; Suganya, S.; Mohandoss, S.; Sudhahar, S. Green inspired synthesis of ZnO nanoparticles and its characterizations with biofilm, antioxidant, anti-inflammatory, and anti-diabetic activities. *J. Mol. Struct.* **2022**, *1255*, 132420, https://doi.org/10.1016/j.molstruc.2022.132420.
12. Siripireddy, B.; Mandal, B.K. Facile green synthesis of zinc oxide nanoparticles by *Eucalyptus globulus* and their photocatalytic and antioxidant activity. *Adv. Powder Technol.* **2017**, *28*, 785–797, https://doi.org/10.1016/j.apt.2016.11.026.
13. Kitture, R.; Chordiya, K.; Gaware, S.; Ghosh, S.; More, P.A.; Kulkarni, P.; Chopade, B.A.; Kale, S.N. ZnO Nanoparticles-Red Sandalwood Conjugate: A Promising Anti-Diabetic Agent. *J. Nanosci. Nanotechnol.* **2015**, *15*, 4046–4051, https://doi.org/10.1166/jnn.2015.10323.
14. Norouzi Jobie, F.; Ranjbar, M.; Hajizadeh Moghaddam, A.; Kiani, M. Green synthesis of zinc oxide nanoparticles using Amygdalus scoparia Spach stem bark extract and their applications as an alternative antimicrobial, anticancer, and anti-diabetic agent. *Adv. Powder Technol.* **2021**, *32*, 2043–2052, https://doi.org/10.1016/j.apt.2021.04.014.
15. Velaga, V.S.A.R.; Suryadevara, N.; Ying, R.T.C.; Ponmurugan, P.; Devi, G. Analgesic activity of Annona squamosa Linn fruit peels on Swis Albino mice. *Res. J. Pharm. Technol.* **2020**, *13*, 3199-3204, https://doi.org/10.5958/0974-360X.2020.00566.1.
16. Ma, C.; Chen, Y.; Chen, J.; Li, X.; Chen, Y. A review on Annona squamosa L.: phytochemicals and biological activities. *Am. J. Chin. Med.* **2017**, *45*, 933-964, https://doi.org/10.1142/S0192415X17500501.
17. Ponrasu, T.; Suguna, L. Efficacy of Annona squamosa on wound healing in streptozotocin-induced diabetic rats. *Int. Wound J.* **2012**, *9*, 613-623, https://doi.org/10.1111/j.1742-481X.2011.00924.x.
18. Oo, W.M.; Khine, M.M. Pharmacological activities of Annona squamosa: Updated. *Chemistry* **2017**, *3*, 86-93, https://doi.org/10.11648/j.ijpc.20170306.14.
19. Safira, A.; Widayani, P.; An-Najaaty, D. A review of an important plants: Annona squamosa leaf. *Phcog. J.* **2022**, *14*, 456-463, https://doi.org/10.5530/pj.2022.14.58.
20. Nguyen, M.; Nguyen, V.; Le, V.; Trieu, L.; Lam, T.; Bui, L.; Nhan, L.; Danh, V. Assessment of preliminary phytochemical screening, polyphenol content, flavonoid content, and antioxidant activity of custard apple leaves (*Annona squamosa* Linn.). *IOP Conf. Ser.: Mater. Sci. Eng.* **2020**, *736*, 062012, https://doi.org/10.1088/1757-899X/736/6/062012.
21. Kumar, M.; Changan, S.; Tomar, M.; Prajapati, U.; Saurabh, V.; Hasan, M.; Sasi, M.; Maheshwari, C.; Singh, S.; Dhumal, S. Custard apple (*Annona squamosa* L.) leaves: Nutritional composition, phytochemical profile, and health-promoting biological activities. *Biomolecules* **2021**, *11*, 614, https://doi.org/10.3390/biom11050614.
22. Shaikh, J.R.; Patil, M. Qualitative tests for preliminary phytochemical screening: An overview. *Int. J. Chem. Stud.* **2020**, *8*, 603-608, https://doi.org/10.22271/chemi.2020.v8.i2i.8834.
23. Badrulhisham, N.S.R.; Ab Hamid, S.N.P.; Ismail, M.A.H.; Yong, Y.K.; Zakuan, N.M.; Harith, H.H.; Saidi, H.I.; Nurdin, A. Harvested locations influence the total phenolic content, antioxidant levels, cytotoxic, and anti-inflammatory activities of stingless bee honey. *J. Asia. Pac. Entomol.* **2020**, *23*, 950-956, https://doi.org/10.1016/j.aspen.2020.07.015.
24. Joshi, S.; Bhattarai, K.; Subedi, A.R.; Bhattarai, J.; Amatya, S.; Baral, B. Validation of ethnopharmacological findings of Aegle marmelos (L.) Correa through phytochemical screening and bioactivity assay. *Pharmacol. Res. Nat. Prod.* **2024**, *5*, 100114, https://doi.org/10.1016/j.prenap.2024.100114.
25. Borrás-Linares, I.; Fernández-Arroyo, S.; Arráez-Roman, D.; Palmeros-Suárez, P.; Del Val-Díaz, R.; Andrade-Gonzáles, I.; Fernández-Gutiérrez, A.; Gómez-Leyva, J.; Segura-Carretero, A. Characterization of phenolic compounds, anthocyanidin, antioxidant and antimicrobial activity of 25 varieties of Mexican Roselle (Hibiscus sabdariffa). *Ind. Crop. Prod.* **2015**, *69*, 385-394, https://doi.org/10.1016/j.indcrop.2015.02.053.
26. Bhandari, L. Isolation of quercetin from flower petals, estimation of total phenolic, total flavonoid and antioxidant activity of the different parts of Rhododendron arboreum smith. *Sci. World* **2015**, *12*, https://doi.org/10.3126/sw.v12i12.13569.

27. Brand-Williams, W.; Cuvelier, M.-E.; Berset, C. Use of a free radical method to evaluate antioxidant activity. *LWT - Food Sci. Technol.* **1995**, *28*, 25-30, https://doi.org/10.1016/S0023-6438(95)80008-5.
28. So, V.; Poul, P.; Oeung, S.; Srey, P.; Mao, K.; Ung, H.; Eng, P.; Heim, M.; Srun, M.; Chheng, C. Bioactive compounds, antioxidant activities, and HPLC analysis of nine edible sprouts in Cambodia. *Molecules* **2023**, *28*, 2874, https://doi.org/10.3390/molecules28062874.
29. Motazedi, R.; Rahaiee, S.; Zare, M. Efficient biogenesis of ZnO nanoparticles using extracellular extract of Saccharomyces cerevisiae: Evaluation of photocatalytic, cytotoxic and other biological activities. *Bioorg. Chem.* **2020**, *101*, 103998, https://doi.org/10.1016/j.bioorg.2020.103998.
30. Xiao, F.; Xu, T.; Lu, B.; Liu, R. Guidelines for antioxidant assays for food components. *Food Front.* **2020**, *1*, 60-69, https://doi.org/10.1002/fft2.10.
31. Lankatillake, C.; Luo, S.; Flavel, M.; Lenon, G.B.; Gill, H.; Huynh, T.; Dias, D.A. Screening natural product extracts for potential enzyme inhibitors: protocols, and the standardisation of the usage of blanks in α-amylase, α-glucosidase and lipase assays. *Plant Methods* **2021**, *17*, 3, https://doi.org/10.1186/s13007-020-00702-5.
32. Chakraborty, S.; Farida, J.J.; Simon, R.; Kasthuri, S.; Mary, N. Averrhoe carrambola fruit extract assisted green synthesis of zno nanoparticles for the photodegradation of congo red dye. *Surfaces and Interfaces* **2020**, *19*, 100488, https://doi.org/10.1016/j.surfin.2020.100488.
33. Selvam, K.; Allam, A.A.; Ajarem, J.S.; Sudhakar, C.; Selvankumar, T.; Senthilkumar, B.; Kim, W. Annona reticulata leaves-assisted synthesis of zinc oxide nanoparticles and assessment of cytotoxicity and photocatalytic impact. *Mater. Lett.* **2022**, *309*, 131379, https://doi.org/10.1016/j.matlet.2021.131379.
34. Ruddaraju, L.K.; Pammi, S.; Pallela, P.V.K.; Padavala, V.S.; Kolapalli, V.R.M. Antibiotic potentiation and anti-cancer competence through bio-mediated ZnO nanoparticles. *Mater. Sci. Eng. C* **2019**, *103*, 109756, https://doi.org/10.1016/j.msec.2019.109756.
35. Esteves, B.; Velez Marques, A.; Domingos, I.; Pereira, H. Chemical changes of heat treated pine and eucalypt wood monitored by FTIR. *Maderas* **2013**, *15*, 245-258, https://doi.org/10.4067/S0718-221X2013005000020.
36. Özgenç, Ö.; Durmaz, S.; Boyaci, I.H.; Eksi-Kocak, H. Determination of chemical changes in heat-treated wood using ATR-FTIR and FT Raman spectrometry. *Spectrochim. Acta A Mol. Biomol. Spectrosc.* **2017**, *171*, 395-400, https://doi.org/10.1016/j.saa.2016.08.026.
37. Upadhyay, P.; Jain, V.K.; Sharma, S.; Shrivastav, A.; Sharma, R. Green and chemically synthesized ZnO nanoparticles: A comparative study. *IOP Conf. Ser.: Mater. Sci. Eng.* **2020**, *798*, 012025, https://doi.org/10.1088/1757-899X/798/1/012025.
38. Al-Darwesh, M.Y.; Ibrahim, S.S.; Mohammed, M.A. A review on plant extract mediated green synthesis of zinc oxide nanoparticles and their biomedical applications. *Results Chem.* **2024**, *7*, 101368, https://doi.org/10.1016/j.rechem.2024.101368.
39. El Omari, N.; Sayah, K.; Fettach, S.; El Blidi, O.; Bouyahya, A.; Faouzi, M.E.A.; Kamal, R.; Barkiyou, M. Evaluation of in vitro antioxidant and antidiabetic activities of Aristolochia longa extracts. *Evid.-Based Complementary Altern. Med.* **2019**, *2019*, 7384735, https://doi.org/10.1155/2019/7384735.
40. Neethu Simon, K.; Santhoshkumar, R.; Neethu, S.K. Phytochemical analysis and antimicrobial activities of Annona squamosa (L) leaf extracts. *J. Pharmacogn. Phytochem.* **2016**, *5*, 128–131.
41. Bitwell, C.; Indra, S.S.; Luke, C.; Kakoma, M.K. A review of modern and conventional extraction techniques and their applications for extracting phytochemicals from plants. *Sci. Afr.* **2023**, *19*, e01585, https://doi.org/10.1016/j.sciaf.2023.e01585.
42. Malta, L.G.; Liu, R.H. Analyses of Total Phenolics, Total Flavonoids, and Total Antioxidant Activities in Foods and Dietary Supplements. In Encyclopedia of Agriculture and Food Systems, Van Alfen, N.K., Ed.; Academic Press: Oxford, **2014**; pp. 305-314, https://doi.org/10.1016/B978-0-444-52512-3.00058-9.
43. Al-Nemari, R.; Al-Senaidy, A.; Semlali, A.; Ismael, M.; Badjah-Hadj-Ahmed, A.Y.; Ben Bacha, A. GC-MS profiling and assessment of antioxidant, antibacterial, and anticancer properties of extracts of Annona squamosa L. leaves. *BMC Complement. Med. Ther.* **2020**, *20*, 296, https://doi.org/10.1186/s12906-020-03029-9.
44. Wanyo, P.; Siriamornpun, S.; Meeso, N. Improvement of quality and antioxidant properties of dried mulberry leaves with combined far-infrared radiation and air convection in Thai tea process. *Food Bioprod. Process.* **2011**, *89*, 22-30, https://doi.org/10.1016/j.fbp.2010.03.005.
45. Najafabad, A.M.; Jamei, R. Free radical scavenging capacity and antioxidant activity of methanolic and ethanolic extracts of plum (Prunus domestica L.) in both fresh and dried samples. *Avicenna J. Phytomed.* **2014**, *4*, 343-353.
46. Uribe, E.; Marín, D.; Vega-Gálvez, A.; Quispe-Fuentes, I.; Rodríguez, A. Assessment of vacuum-dried peppermint (Mentha piperita L.) as a source of natural antioxidants. *Food Chem.* **2016**, *190*, 559-565, https://doi.org/10.1016/j.foodchem.2015.05.108.
47. Shi, L.; Zhao, W.; Yang, Z.; Subbiah, V.; Suleria, H.A.R. Extraction and characterization of phenolic compounds and their potential antioxidant activities. *Environ. Sci. Pollut. Res.* **2022**, *29*, 81112-81129, https://doi.org/10.1007/s11356-022-23337-6.

48. Sharma, K.; Ko, E.Y.; Assefa, A.D.; Ha, S.; Nile, S.H.; Lee, E.T.; Park, S.W. Temperature-dependent studies on the total phenolics, flavonoids, antioxidant activities, and sugar content in six onion varieties. *J. Food Drug Anal.* **2015**, *23*, 243-252, https://doi.org/10.1016/j.jfda.2014.10.005.
49. Ma, Y.-Q.; Chen, J.-C.; Liu, D.-H.; Ye, X.-Q. Simultaneous extraction of phenolic compounds of citrus peel extracts: Effect of ultrasound. *Ultrason. Sonochem.* **2009**, *16*, 57-62, https://doi.org/10.1016/j.ultsonch.2008.04.012.
50. Shraim, A.M.; Ahmed, T.A.; Rahman, M.M.; Hijji, Y.M. Determination of total flavonoid content by aluminum chloride assay: A critical evaluation. *LWT* **2021**, *150*, 111932, https://doi.org/10.1016/j.lwt.2021.111932.
51. Wan, C.; Yu, Y.; Zhou, S.; Liu, W.; Tian, S.; Cao, S. Antioxidant activity and free radical-scavenging capacity of Gynura divaricata leaf extracts at different temperatures. *Pharmacogn. Mag.* **2011**, *7*, 40, https://doi.org/10.4103/0973-1296.75900.
52. Mehar, S.; Khoso, S.; Qin, W.; Anam, I.; Iqbal, A.; Iqbal, K. Green Synthesis of Zinc oxide Nanoparticles from Peganum harmala, and its biological potential against bacteria. *Front. Nanosci. Nanotech* **2019**, *6*, 1-5, https://doi.org/10.15761/FNN.1000188.
53. Pourrahimi, A.M.; Liu, D.; Pallon, L.K.; Andersson, R.L.; Abad, A.M.; Lagarón, J.-M.; Hedenqvist, M.S.; Ström, V.; Gedde, U.W.; Olsson, R.T. Water-based synthesis and cleaning methods for high purity ZnO nanoparticles–comparing acetate, chloride, sulphate and nitrate zinc salt precursors. *RSC Adv.* **2014**, *4*, 35568-35577, https://doi.org/10.1039/C4RA06651K.
54. Senguttuvan, J.; Paulsamy, S.; Karthika, K. Phytochemical analysis and evaluation of leaf and root parts of the medicinal herb, Hypochaeris radicata L. for in vitro antioxidant activities. *Asian Pacific journal of tropical biomedicine* **2014**, *4*, S359-S367, https://doi.org/10.12980/APJTB.4.2014C1030.
55. Verma, R.; Kumar, D.; Nagraik, R.; Sharma, A.; Tapwal, A.; Puri, S.; Kumar, H.; Kumari, A.; Nepovimova, E.; Kuca, K. Mycorrhizal inoculation impact on Acorus calamus L.-An ethnomedicinal plant of western Himalaya and its in silico studies for anti-inflammatory potential. *J. Ethnopharmacol.* **2021**, *265*, 113353, https://doi.org/10.1016/j.jep.2020.113353.
56. Dhatwalia, J.; Kumari, A.; Chauhan, A.; Mansi, K.; Thakur, S.; Saini, R.V.; Guleria, I.; Lal, S.; Kumar, A.; Batoo, K.M. Rubus ellipticus Sm. Fruit extract mediated zinc oxide nanoparticles: a green approach for dye degradation and biomedical applications. *Materials* **2022**, *15*, 3470, https://doi.org/10.3390/ma15103470.
57. Liang, T.; Yue, W.; Li, Q. Comparison of the phenolic content and antioxidant activities of Apocynum venetum L.(Luo-Bu-Ma) and two of its alternative species. *Int. J. Mol. Sci.* **2010**, *11*, 4452-4464, https://doi.org/10.3390/ijms11114452.
58. Rabeta, M.S.; Lin, S.P. Effects of Different Drying Methods on the Antioxidant Activities of Leaves and Berries of *Cayratia trifolia*. *Sains Malays* **2015**, *44*, 275–280, https://doi.org/10.17576/jsm-2015-4402-16.
59. Hossain, M.; Barry-Ryan, C.; Martin-Diana, A.B.; Brunton, N. Effect of drying method on the antioxidant capacity of six Lamiaceae herbs. *Food Chem.* **2010**, *123*, 85-91, https://doi.org/10.1016/j.foodchem.2010.04.003.
60. Cai, Y.-Z.; Sun, M.; Xing, J.; Luo, Q.; Corke, H. Structure–radical scavenging activity relationships of phenolic compounds from traditional Chinese medicinal plants. *Life Sci.* **2006**, *78*, 2872-2888, https://doi.org/10.1016/j.lfs.2005.11.004.
61. La, J.; Kim, M.-J.; Lee, J. Evaluation of solvent effects on the DPPH reactivity for determining the antioxidant activity in oil matrix. *Food Sci. Biotechnol.* **2021**, *30*, 367-375, https://doi.org/10.1007/s10068-020-00874-9.
62. Hanh, N.H.; Nguyet, Q.T.M.; Van Chinh, T.; Duong, L.D.; Tien, T.X.; Van Duy, L.; Hoa, N.D. Enhanced photocatalytic efficiency of porous ZnO coral-like nanoplates for organic dye degradation. *RSC Adv.* **2024**, *14*, 14672-14679, https://doi.org/10.1039/D4RA01345J.
63. Shabaani, M.; Rahaiee, S.; Zare, M.; Jafari, S.M. Green synthesis of ZnO nanoparticles using loquat seed extract; Biological functions and photocatalytic degradation properties. *LWT* **2020**, *134*, 110133, https://doi.org/10.1016/j.lwt.2020.110133.
64. Lal, S.; Verma, R.; Chauhan, A.; Dhatwalia, J.; Guleria, I.; Ghotekar, S.; Thakur, S.; Mansi, K.; Kumar, R.; Kumari, A. Antioxidant, antimicrobial, and photocatalytic activity of green synthesized ZnO-NPs from Myrica esculenta fruits extract. *Inorg. Chem. Commun.* **2022**, *141*, 109518, https://doi.org/10.1016/j.inoche.2022.109518.
65. Jayakar, V.; Lokapur, V.; Nityasree, B.R.; Chalannavar, R.K.; Lasrado, L.D.; Shantaram, M. Optimization and green synthesis of zinc oxide nanoparticle using Garcinia cambogia leaf and evaluation of their antioxidant and anticancer property in kidney cancer (A498) cell lines. *Biomedicine* **2021**, *41*, 206–222, https://doi.org/10.51248/.v41i2.785.
66. Bhalodia, N.R.; Nariya, P.B.; Acharya, R.; Shukla, V. In vitro antioxidant activity of hydro alcoholic extract from the fruit pulp of Cassia fistula Linn. *AYU* **2013**, *34*, 209-214, https://doi.org/10.4103/0974-8520.119684.

67. Chou, S.T.; Chao, W.W.; Chung, Y.C. Antioxidative activity and safety of 50% ethanolic red bean extract (Phaseolus radiatus L. var. Aurea). *J. Food Sci.* **2003**, *68*, 21-25, https://doi.org/10.1111/j.1365-2621.2003.tb14108.x.
68. Vikas, B.; Akhil, B.; Remani, P.; Sujathan, K. Free radical scavenging properties of Annona squamosa. *Asian Pac. J. Cancer Prev.* **2017**, *18*, 2725, https://doi.org/10.22034/APJCP.2017.18.10.2725.
69. Cerretani, L.; Bendini, A. Chapter 67 - Rapid Assays to Evaluate the Antioxidant Capacity of Phenols in Virgin Olive Oil. In Olives and Olive Oil in Health and Disease Prevention, Preedy, V.R., Watson, R.R., Eds.; Academic Press: San Diego, **2010**; pp. 625-635, https://doi.org/10.1016/B978-0-12-374420-3.00067-X.
70. Hammoud, S.; Jaber, A.; Ibrahim, G.; Cheble, E. Storage Effect On The Gc-Ms Profiling And Antioxidant Activities Of Essential Oils From Leaves Of Annona Squamosa L. *Univers. J. Pharm. Res.* **2022**, *7*, 51-57, https://doi.org/10.22270/ujpr.v7i3.785.
71. Kalidindi, N.; Thimmaiah, N.V.; Jagadeesh, N.V.; Nandeep, R.; Swetha, S.; Kalidindi, B. Antifungal and antioxidant activities of organic and aqueous extracts of Annona squamosa Linn. leaves. *J. Food Drug Anal.* **2015**, *23*, 795-802, https://doi.org/10.1016/j.jfda.2015.04.012.
72. Kozłowska, M.; Ścibisz, I.; Przybył, J.; Ziarno, M.; Żbikowska, A.; Majewska, E. Phenolic contents and antioxidant activity of extracts of selected fresh and dried herbal materials. *Pol. J. Food Nutr. Sci.* **2021**, *71*, 269-278, https://doi.org/10.31883/pjfns/139035.
73. Pulido, R.; Bravo, L.; Saura-Calixto, F. Antioxidant activity of dietary polyphenols as determined by a modified ferric reducing/antioxidant power assay. *J. Agric. Food Chem.* **2000**, *48*, 3396-3402, https://doi.org/10.1021/jf9913458.
74. Alam, U.; Asghar, O.; Azmi, S.; Malik, R.A. Chapter 15 - General aspects of diabetes mellitus. In Handbook of Clinical Neurology, Zochodne, D.W., Malik, R.A., Eds.; Elsevier: **2014**; Volume 126, pp. 211-222, https://doi.org/10.1016/B978-0-444-53480-4.00015-1.
75. Dirir, A.M.; Daou, M.; Yousef, A.F.; Yousef, L.F. A review of alpha-glucosidase inhibitors from plants as potential candidates for the treatment of type-2 diabetes. *Phytochem. Rev.* **2022**, *21*, 1049-1079, https://doi.org/10.1007/s11101-021-09773-1.
76. Levetan, C. Oral antidiabetic agents in type 2 diabetes. *Curr. Med. Res. Opin.* **2007**, *23*, 945-952, https://doi.org/10.1185/030079907X178766.
77. Przeor, M. Some common medicinal plants with antidiabetic activity, known and available in Europe (A Mini-Review). *Pharmaceuticals* **2022**, *15*, 65, https://doi.org/10.3390/ph15010065.
78. Nkemzi, A.Q.; Okaiyeto, K.; Oyenihi, O.; Opuwari, C.S.; Ekpo, O.E.; Oguntibeju, O.O. Antidiabetic, anti-inflammatory, antioxidant, and cytotoxicity potentials of green-synthesized zinc oxide nanoparticles using the aqueous extract of helichrysum cymosum. *3 Biotech* **2024**, *14*, 291, https://doi.org/10.1007/s13205-024-04125-0.
79. de Souza, P.M.; de Sales, P.M.; Simeoni, L.A.; Silva, E.C.; Silveira, D.; de Oliveira Magalhães, P. Inhibitory activity of α-amylase and α-glucosidase by plant extracts from the Brazilian cerrado. *Planta Med.* **2012**, *78*, 393-399, https://doi.org/10.1055/s-0031-1280404.
80. Kazeem, M.; Dansu, T.; Adeola, S. Inhibitory effect of Azadirachta indica A. Juss leaf extract on the activities of cz-amylase and oz-glucosidase. *Pak. J. Biol. Sci.* **2013**, *16*, 1358-1362, https://doi.org/10.3923/pjbs.2013.1358.1362.

Publisher's Note & Disclaimer

Supplementary Materials

(a)

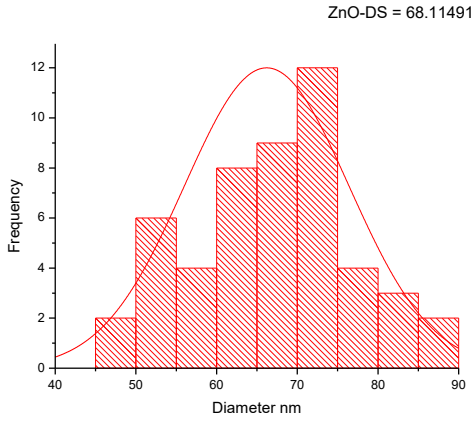

(b)

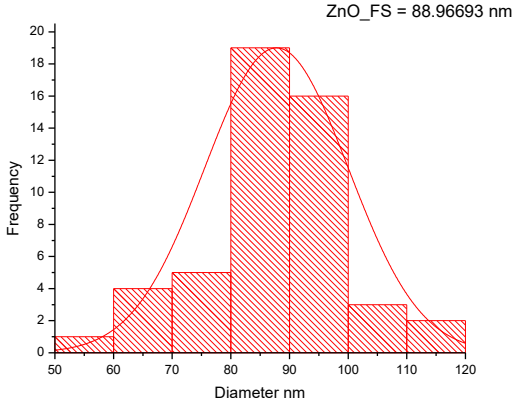

(c)

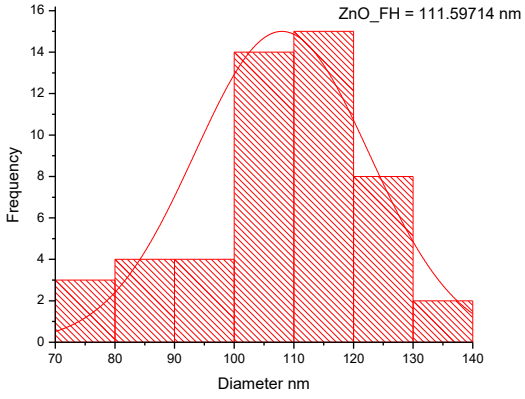

Figure S1. SEM particle distribution histogram graphs for (a) ZnO-DS, (b) ZnO-FS, and (c) ZnO-FH.

Table S1. XRD peak lists for ZnO-FS (a), ZnO-DS (b) and ZnO-FH (c).

(a)

Pos. [°2θ]	Height [cts]	FWHM [°2θ]	d-spacing [Å]	Rel. Int. [%]
11.3959	0.06	1.8893	7.76495	0.12
31.8261	36.59	0.6298	2.81181	65.11
34.5106	28.74	0.6298	2.59898	51.14
36.2571	56.20	0.6298	2.47770	100.00
47.6098	14.54	0.7872	1.91004	25.88
56.6865	25.55	0.6298	1.62387	45.47
62.9866	16.32	0.6298	1.47576	29.04
68.0270	14.28	0.7872	1.37818	25.41
77.0700	1.62	2.3040	1.23645	2.88

(b)

Pos. [°2θ]	Height [cts]	FWHM [°2θ]	d-spacing [Å]	Rel. Int. [%]
28.3930	11.99	0.2362	3.14350	29.78
29.5070	11.59	0.6298	3.02730	28.79
31.8405	25.18	0.9446	2.81057	62.55
34.5328	19.17	0.6298	2.59736	47.63
36.2616	40.25	0.3936	2.47741	100.00
39.6073	2.71	0.4723	2.27551	6.74
40.5969	8.43	0.2362	2.22229	20.95
47.6219	11.02	0.6298	1.90958	27.37
56.7025	14.60	1.1021	1.62345	36.26
62.9709	13.13	0.6298	1.47609	32.63
68.1063	9.63	0.7872	1.37677	23.93
77.1857	1.31	1.5360	1.23488	3.25

(c)

Pos. [°2θ]	Height [cts]	FWHM [°2θ]	d-spacing [Å]	Rel. Int. [%]
10.6673	0.23	0.9446	8.29363	0.49
28.4295	8.99	0.2362	3.13955	18.71
29.5424	12.42	0.6298	3.02376	25.85
31.8806	27.42	0.6298	2.80713	57.10
34.5782	21.73	0.6298	2.59406	45.26
36.3737	48.02	0.7872	2.47003	100.00
40.6160	3.32	0.4723	2.22129	6.92
43.3737	3.34	0.4723	2.08624	6.96
47.6143	13.19	0.7872	1.90987	27.48
56.7104	14.91	0.9446	1.62324	31.06
63.0018	12.75	0.9446	1.47544	26.56
68.0675	10.43	0.7872	1.37746	21.72
77.0241	2.05	1.1520	1.23707	4.28

(a)

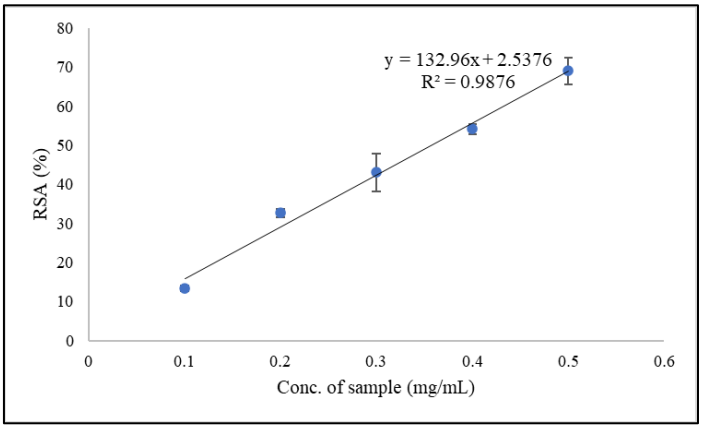

(b)

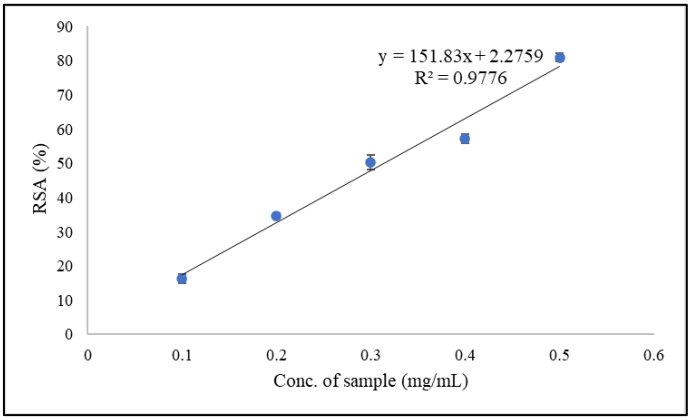

(c)

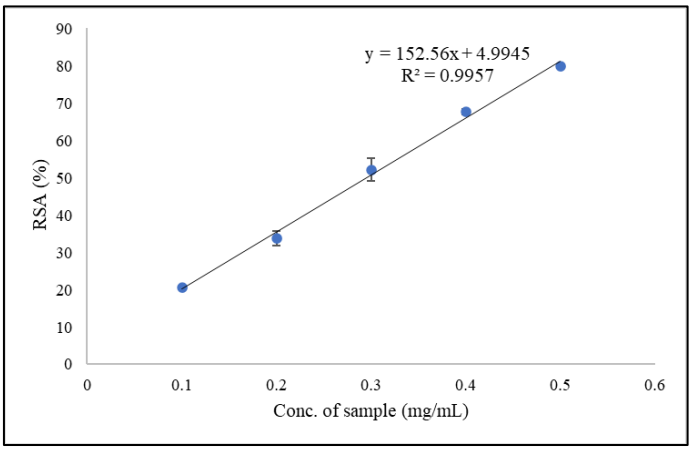

Figure S2. Radical scavenging activity (%) of (a)LE-FH, (b) of LE-FS and (c) LE-DS from 0.1 – 0.5 mg/mL.